ORIGINAL PAPER

# Translational and Rotational Motions of Albumin Sensed by a Non-Covalent Associated Porphyrin Under Physiological and Acidic Conditions: A Fluorescence Correlation Spectroscopy and Time Resolved Anisotropy Study

**Suzana M. Andrade · Silvia M. B. Costa · Jan Willem Borst · Arie van Hoek · Antonie J. W. G. Visser**

**Abstract** The interaction between a free-base, anionic water-soluble porphyrin, TSPP, and the drug carrier protein, bovine serum albumin (BSA) has been studied by time-resolved fluorescence anisotropy (TRFA) and fluorescence correlation spectroscopy (FCS) at two different pH-values. Both rotational correlation times and translational diffusion times of the fluorescent species indicate that TSPP binding to albumin induces very little conformational changes in the protein under physiological conditions. By contrast, at low pH, a bi-exponential decay is obtained where a short rotational correlation time ($\phi_{int}=1.2$ ns) is obtained, which is likely associated to wobbling movement of the porphyrin in the protein binding site. These physical changes are corroborated by circular dichroism (CD) data which show a 37% loss in the protein helicity upon acidification of the medium. In the presence of excess porphyrin formation of porphyrin J-aggregates is induced, which can be detected by time-resolved fluorescence with short characteristic times. This is also reflected in FCS data by an increase in molecular brightness together with a decrease in the number of fluorescent molecules passing through the detection volume of the sample.

## Introduction

The induced structural changes upon ligand binding have been a matter of extensive studies and modeling since biologic processes are carried out through binding events, changes in the environment and signaling pathways [1–3].

Binding influences distribution, metabolism and the molecular form of the sensitizers, e.g. their protonation state, aggregation/dis-aggregation behavior and the concentration of the free molecules. Binding can also alter their photophysical and photochemical properties [4, 5]. Hence, it is important to investigate how and to which extent it influences the photosensitized reactions. Conversely, upon binding, ligands can induce structural modifications in the proteins [6–8].

Proteins have single or multiple binding sites for porphyrinoids, including independent cooperative modes. In particular, the serum albumin, constituting about 60% of the total amount of protein in plasma, is known to serve as an endogenous carrier for various drugs, particularly those that are relatively hydrophilic which bind to two well-defined

S. M. Andrade (✉) · S. M. B. Costa
Centro de Química Estrutural, Complexo 1,
Instituto Superior Técnico,
1049-001 Lisbon, Portugal
e-mail: suzana.andrade@ist.utl.pt

J. W. Borst · A. van Hoek · A. J. W. G. Visser
Wageningen University, MicroSpectroscopy Centre,
6703 HA Wageningen, The Netherlands

binding sites I and II [9]. The large plasticity of human serum albumin (HSA) is essential for the albumin molecule to accommodate a variety of ligands and to perform the transport function in the circulatory system. Besides, it is known that HSA undergoes reversible conformational isomerization upon pH-change [10]. Since different acidic and basic isomers may have determined biological functions we have conducted our experiments both at pH=7.4 and pH=2.5. The complexes of porphyrinoids with serum albumin are believed to be stabilized by electrostatic interactions between negatively charged substituents on the molecular periphery and positively charged ammonium residues on serum albumins.

We have previously shown [11] that the anionic water-soluble porphyrin, *meso*-tetrakis (*p*-sulfonatophenyl) porphyrin sodium salt—TSPP, binds to albumins with relatively high binding constants, ($K_B \sim 3$–$5 \times 10^6$ M$^{-1}$) where electrostatic and hydrophobic interactions are involved. Moreover, under acidic conditions TSPP is prevalently present in solution as a zwitterion. This has proved to contribute decisively to the formation of highly ordered molecular aggregates of the porphyrin at relatively low [TSPP] induced by different polymeric templates [12–14] including albumins [11, 15]. These aggregates of J-type are particularly interesting in view of their possible applications in nonlinear optics, nanometer-sized photoconductors, and light harvesting systems and contributed also for the relevance of the studies carried on at pH=2.5.

In order to further characterize the porphyrin–albumin interactions we have used fluorescence correlation spectroscopy (FCS). FCS has emerged as an important technique in biophysical studies to study diffusion as well as conformational and chemical transitions on microsecond and longer timescales [16, 17]. The technique is a highly sensitive tool to measure concentration and diffusion coefficients from which we may determine binding/dissociation equilibria in the nanomolar range [18]. These results were complemented by time-resolved fluorescence anisotropy (TRFA), by which the time-correlation function of the emission transition moment is determined. The conjugation of these two techniques is expected to provide further insight concerning the molecular dynamics of TSPP–BSA interaction.

The results obtained indicate that under physiological conditions TSPP binding to albumin induces very little conformational changes in the protein, whereas at low pH both translational and rotational diffusion coefficients diverge from those at pH=7.4 and the porphyrin is more free to rotate itself in the binding site. Consistent with acid denaturation of proteins [19], the results point to a loss in the protein tertiary and secondary structure at pH=2.5, which is partially regained in the presence of an equimolar amount of TSPP.

## Experimental

*Materials* BSA ≥ 97% purity (catalogue no. A-7511) was purchased from Sigma and used without further purification. TSPP was obtained from Fluka ≥98% purity (catalogue no. 88074). Citrate-phosphate buffer solutions (pH= 2.5 and 7.4, 25 mM) were made up using bidistilled water, following the recommended procedures [20]. In all experiments we used fresh stock solutions of protein.

*Methods* Circular Dichroism (CD) measurements were performed on a Jasco J-720 spectropolarimeter (Hachioji City, Tokyo). The protein concentration and path lengths of quartz cells used for the far-UV CD experiments were 5 μM and 0.1 cm, respectively. The spectropolarimeter was thoroughly purged with 99.9% nitrogen before starting the instrument. Each spectrum was baseline-corrected, and the final plot was taken as an average of ten accumulated plots. The CD signal (in mdeg) was converted to mean residual ellipticity ($\theta$; deg.cm$^2$.dmol$^{-1}$) defined as $(\theta)=\theta_{obs}(10cln)^{-1}$, where $\theta_{obs}$ (mdeg) is the experimental ellipticity, $c$ (mol.dm$^{-3}$) is the protein concentration, $l$ (cm) is the cell path length, and $n$ is the number of residues in the protein [21].

Time-resolved (polarized) fluorescence measurements were carried out using a setup described elsewhere [22]. The excitation wavelengths used were 430 nm and 480 nm and the fluorescence was detected through band-pass filters with maximum transmission at 647 nm and 713 nm ($\Delta\lambda$= 13 nm). Decay traces were fitted to a sum of exponentials, with the TRFA Data Processing Package (version 1.2) of the Scientific Software Technologies Center (Belarusian State University, Minsk, Belarus; www.sstcenter.com) [23]. Typical probe concentrations were 0.5 μM.

Dilute porphyrin samples (in the range of 1–10 nM) were investigated by FCS using a commercial set-up from PicoQuant based on an inverted optical microscope (Olympus IX-71). The 638 nm excitation light from a pulsed diode laser was focused by an oil immersion objective ×100 with 1.3 NA, ~20 μm deep into the sample solution. Fluorescence is collected by the same microscope objective, passed through the dichroic mirror and appropriate band-pass filter (695AF55 Omega optical) and focused through a pinhole (150 μm), to reject out-of-focus light, onto a single-photon counting avalanche photodiode SPAD (Perkin-Elmer) whose signal was processed by TimeHarp 200 time-correlated single-photon counting card (PicoQuant). Focal area and detection volume were calibrated using Atto 655 dye in the carboxylic acid form (Atto-Tech GmbH, Germany) with known diffusion coefficient $D=4.26\times10^{-10}$ m$^2$ s$^{-1}$ [24]. Data analysis of individual correlation curves was performed using SymPhoTime (PicoQuant) and a programmed global fitting analysis was carried out in Microsoft® Excel.

The temperature of the experiments was stabilized at 22 °C.

## Results and discussion

*Circular dichroism spectroscopy* The changes in the secondary structures of the protein in the presence of TSPP were studied in the far-UV CD region at increasing molar ratios of [TSPP]/[BSA] at two different pHs, Fig. 1a. The spectrum of intact BSA at pH=7.4 showed two minima at 209 and 222 nm, which is in agreement with the literature [25], and reflects the predominance of a secondary α-helix structure for BSA (~65%). In the presence of TSPP, initially the CD spectrum becomes more negative reaching the minimum at a 1:1 protein to porphyrin ratio. We can exclude contribution from TSPP to this signal since, taking into account the absence of chirality in TSPP molecules, as expected no CD signal was detected for TSPP samples without BSA in the UV-Vis range. Nevertheless, an intense induced CD arising from the chiral packing of the molecules into large aggregates was detected in the visible range [11]. At higher ratios, the signal is less negative. The spectrum for BSA at pH=2.5 shows a large decrease in the mean molar residue ellipticity (θ), which points to a substantial loss in native structure under acidic conditions. Nevertheless, the TSPP presence contributes to a more negative (θ) which reaches a minimum at 1:1 protein to porphyrin ratio, similarly to pH=7.4.

The α-helical content was estimated from the molar ellipticity value at 222 nm, $[\theta]_{222nm}$, taking into account an helix length-dependent factor according to [26], with $n$ the number of residues in the protein:

$$\alpha - \text{helix}(\%) = \frac{(\theta)_{222nm}}{-39,500 \times (1 - 2.57/n)} \times 100 \qquad (1)$$

The values obtained for the α-helix content at the different protein to porphyrin ratios at the two distinct pHs are depicted in Fig. 1b. Basically, they confirm an almost 32% loss in helical content for BSA upon acidification. This structural alteration is due to repulsive forces acting below its isoelectric point ($pI_{BSA} \sim 5$) within the highly charged protein. It was shown elsewhere [27] that these alterations involved a decrease in compressibility and volume of the protein. The loss in helices leads to exposure of the protein surface to the aqueous environment and at the same time contributes to the collapse of some cavities. CD measurements showed that these are essentially associated to structural changes in the C-terminal domain III of HSA and involved disruption of intradomain contacts (of domain III) within the limits of the disulfide bridges [25].

Recently, this expanded state has been attributed to a molten globule-like state for albumin at low pH, according to the accepted general definition: presence of native-like secondary structure, a fluctuating tertiary structure, non-cooperative thermal unfolding [28, 29], clearly distinguishable from the GdnHCl-denatured state [19]. In order to assimilate and release molecules of quite distinct size/shape in the circulatory system, HSA has to possess a flexible structure. This was positively inferred from changes in the solvation dynamics of HSA, using the single tryptophan fluorescence as reporter, which correlated with the conformational transitions that occur upon pH changes [30].

The presence of low amounts of TSPP lead to an almost recovery of native like helices at pH=2.5 and to a further increase at pH=7.4, which is in agreement with data obtained from X-ray [31] that evidences important structural changes upon ligand binding.

It has been reported that proteins that are extensively unfolded at pH 2 have been observed to regain some native structure in the presence of ions [32]. In fact, salt-dependent refolding of acid-denatured proteins is primarily attributed to anion binding. It is likely that electrostatic interactions between anions and the protonated sites on the protein molecule provide a shielding effect on the repulsive positive charges, thus allowing the protein to adopt a more native-like conformation. Also 1,8-ANS binding to albumin in the acidic expanded conformation induces shrinkage of the hydrodynamic volume of the protein [33]. Although at pH=7.4 the global charge of albumin is negative and TSPP is tetra-anionic, the local charge of the homologous binding
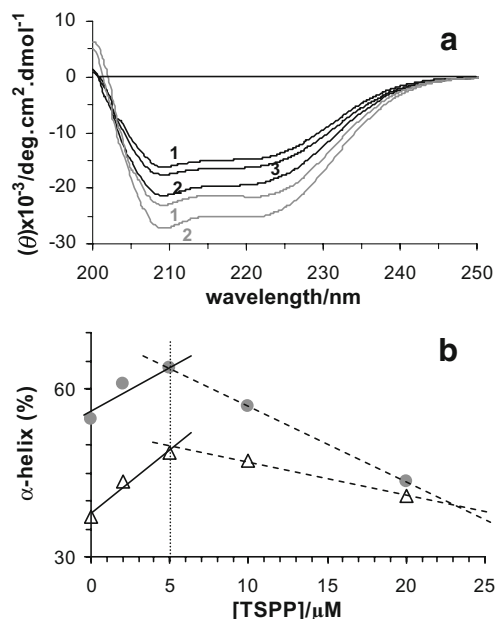


Fig. 1 **a** CD spectra of BSA (5 μM) in aqueous solution at pH=2.5 (*black lines*) and at pH=7.4 (*grey lines*) in the presence of different [TSPP]: *1* 0; *2* 5 μM; *3* 20 μM. **b** % of α-helix obtained using Eq. 1 for BSA in the presence of different [TSPP] at pH=2.5 (*triangle*) and pH=7.4 (*circle*)

sites in domains IIA and IIIA are positive due to the existence of lysine and arginine residues. Hence, TSPP binding to BSA is electrostatically favorable and may lead to further stabilization of the protein conformation. It was also found that TSPP presence contributes to the stabilization of albumin towards thermal and chemical denaturation by the chaotropic agent guanidine hydrochloride (data not published).

At higher amounts of TSPP, the protein seems to behave in a similar way at both pHs, i.e. a concomitant decrease in α-helix occurs as [TSPP] increases. In fact, at 20 μM the % of α-helix in BSA is almost pH independent. Under these conditions, the balance between electrostatic and hydrophobic mutual interactions is affected in a way that porphyrin–porphyrin interactions are favored over those between porphyrin–protein, thus leading to the decrease in the contents of α-helical structure in the protein.

*Time-resolved fluorescence* The fluorescence lifetime decays of the $Q$-state of TSPP alone and in the presence of different [BSA] at pH=2.5 and 7.4 were analyzed by picosecond single-photon timing ($\lambda_{exc} \approx 430$ or 480 nm), and the results are listed in Table 1. In the case of TSPP alone, emission decays show a biexponential behavior at both pHs with a prevalent long lifetime of 3.78 ns for the di-protonated species (whose contribution depends on emission wavelength) and 9.58 ns for the tetra-anionic one in good agreement with reported values [34–36]. The existence of a sub-nanosecond component had already been reported by others for the aqueous system [13] and attributed to the aggregation of this porphyrin, most probably smaller or less organized aggregates or even a mixture of H- and J-dimers [34], which in the present case, would be induced by the increased ionic strength of the buffered media.

At high [BSA]/[TSPP], a long lifetime of ~12 ns was obtained common to the two pHs, although its contribution depends on excitation/emission wavelengths under acidic conditions. Since the two albumins, HSA and BSA present closely homologous structures and have the same isoelectric point [27], we have taken into account the binding constants already determined for TSPP interaction with HSA, $K_b \sim 5 \times 10^6$ M$^{-1}$ and $K_b \sim 1 \times 10^6$ M$^{-1}$ respectively at pH=2 and pH= 7 [11], from which a fraction of bound TSPP of 85% at the former and 67% at the latter pH, could be withdrawn. These values match reasonably the amplitudes obtained for the long component and therefore, can be assigned to TSPP monomer/BSA complex where the porphyrin is in a hydrophobic environment of the protein matrix and hence "protected" from changes in the solution pH.

By contrast, at low [BSA]/[TSPP] and pH=2.5, the fluorescence decays could only be fitted with a sum of three exponentials at any excitation/emission conditions. The long component, just assigned to the porphyrin–protein complex, has a relatively small contribution to the overall emitting population as expected (fraction of TSPP bound never exceeded 8% under these conditions, see Table 1). The intermediate lifetime can be safely assigned to the di-protonated monomer whose fluorescence overlaps that of the other species. The shortest component of 50 ps corresponds to the aggregated J-form of TSPP and therefore, prevails upon excitation at 480 nm and/or emission at 713 nm. This short component had previously been reported in aqueous solution at very low pH (<1) and higher porphyrin concentration (ca 10$^{-4}$ M) [37] and in the presence of CTAB [12]. The existence of a rich positively charged surface in BSA contributes to favor TSPP aggregation in a head-to-tail configuration by minimizing repulsions between neighboring sulfonate groups in the linear array of TSPP molecules. As [BSA] increases this

**Table 1** Fluorescence lifetimes of TSPP (0.7 μM) in aqueous solution at different pH and in the presence of different [BSA]

| Sample | $A_1$ | $\tau_1$/ns | $A_2$ | $\tau_2$/ns | $A_3$ | $\tau_3$/ns | $\chi^2$ |
|---|---|---|---|---|---|---|---|
| TSPP, pH=2.5 | 0.35 | 0.18 | 0.65 | 3.78 | – | – | 1.042 |
| | 0.04[a] | 0.18[a] | 0.96[a] | 3.78[a] | – | – | 1.071 |
| TSPP, pH=7.4 | 0.34 | 0.32 | 0.66 | 9.58 | – | – | 1.050 |
| [BSA]/[TSPP] = 0.03 pH=2.5 | 0.35 | 0.18 | 0.57 | 3.67 | 0.08 | 10.05 | 1.045 |
| | 0.49[a] | 0.050[a] | 0.49[a] | 3.72[a] | 0.02[a] | 10.20[a] | 1.130 |
| | 0.67[b] | 0.050[b] | 0.32[b] | 3.80[b] | 0.01[b] | 12.25[b] | 1.150 |
| [BSA]/[TSPP] = 10 pH=2.5 | 0.31 | 0.191 | 0.10 | 3.63 | 0.59 | 11.96 | 1.045 |
| | – | – | 0.15[a] | 3.63[a] | 0.85[a] | 11.96[a] | 1.039 |
| | 0.40[b] | 0.050[b] | 0.09[b] | 3.80[b] | 0.51[b] | 12.25[b] | 1.01 |
| [BSA]/[TSPP]=10 pH=7.4 | 0.30 | 0.26 | – | – | 0.70 | 11.68 | 1.054 |

$\lambda_{exc}$=430 nm, $\lambda_{em}$=647 nm; $\Delta\tau_i$ =3%

[a] exc=430 nm/em=713 nm

[b] exc=480 nm/em=713 nm

arrangement is destabilized by competing interactions provided by the protein binding sites, namely binding site I and II (subdomains IIA and IIIA) where ion (dipole)–dipole, van der Waals, and/or H-bonding interactions with the polar cationic groups (e.g. lysine and arginines) as well as hydrophobic interactions with leucine and alanine residues are involved [10].

*Fluorescence anisotropy* In order to focus on the interaction between porphyrin and BSA, time-resolved fluorescence anisotropy experiments were carried out under different pH and [BSA]. These experiments provide information useful to identify the characteristics of the electronic states of excitation and emission through $r_o$, the anisotropy in the absence of rotational diffusion, and the reorientation dynamics of the molecule/aggregate/complex through $r(t)$, the fluorescence anisotropy decay. In aqueous buffered solution $r(t)$ is a single exponential,

$$r(t) = r_0 \exp(-t/\phi) \qquad (2)$$

where $\phi$ is the rotational correlation time. The values obtained for TSPP at pH=2.5 and pH=7.4, 0.462 ns and 0.400 ns, respectively (Table 2), are in good agreement with literature [12] and confirm the monomeric nature of the dye in solution. The rotational correlation time can be related to the hydrodynamic volume ($V$) of the fluorophore and viscosity ($\eta$) by the Stokes–Einstein equation: $\phi = \eta V/kT$. The hydrodynamic volumes of organic molecules can be determined using Edward's theory for the calculation of molecular volume and Perrin's correction for the non-spherical shape of the molecule. The hydrodynamic volume for TSPP is 775 Å$^3$ [34] which corresponds well to a rotational diffusion of 0.44 ns.

In the presence of large amounts of BSA, TSPP exists essentially bound to the protein at both pHs to which corresponds a long fluorescence lifetime. The fluorescence anisotropy decay of a dye molecule bound to a protein is a consequence of the reorientation dynamics of the excited state of the dye as well as of the protein. Nevertheless, the anisotropy decays obtained upon excitation at 430 nm and independently of the detection wavelength (around 648 or 713 nm) are mono-exponential with $\phi = 46 \pm 10$ ns (Fig. 2a) and $\phi = 20 \pm 2$ ns, respectively at pH=7.4 and pH=2.5 (Table 2). Hence, in this case we may assume that the dye molecule is "rigidly attached" to the protein binding site and the orientation dynamics for the molecule is identical to that of the protein.

In view of the available time window of the experiments (20 ns) there is a high inaccuracy involved in the rotational correlation times. Moreover, the fluorescence lifetime of the complex is shorter than the rotational time. To circumvent this difficulty and expand the time window, extrinsic probes with very long lifetime (~800 ns) were used linked to HSA [38] or phosphorescence depolarization methods [39] were applied which contributed to a more accurate value for the rotational time of BSA ca. 42 ns. Data involving the time-resolved depolarization of the intrinsic fluorescence of tryptophan in HSA [40, 41] showed a slow component (34–40 ns) corresponding to the global Brownian rotation of the protein. In spite of some inaccuracy also involved in this last value due to the relatively short average fluorescence lifetime of tryptophan ($<\tau_F>$ 3 ns), these findings are indicative of the absence of internal motions of certain domains in the protein in this time scale and similar to ours. Hence, it is feasible to assign the rotation correlation time of ~46 ns to the motion of the entire native protein. Besides the factors just mentioned such as distinct environmental conditions (e.g.: temperature, ionic strength) may well justify the differences with literature data (less than 12%). At neutral pH, therefore, the protein maintains a well-defined overall conformation without signs of large domain flexibility over a time range from nanoseconds to fractions of milliseconds. The shorter rotational time of 20 ns obtained at pH=2.5 cannot be attributed to the motion of the protein as a whole. One hypothesis is that it could be due to mobility of a large segment of the polypeptide chain in the vicinity of TSPP binding site. However, in acid solution, the compact HSA structure unfolds to a more extended one, as proposed elsewhere [19] which is no longer spherical (rather an elongated ellipsoid [42]) and the observed motion of the protein may be the average of different rotational relaxation times along various axes.

By contrast, at the same high [BSA]/[TSPP] but upon excitation at 480 nm, the anisotropy decays are no longer single exponential (Fig. 2b) indicating that additional depolarization processes occur along the duration of the measurement. A long correlation time still predominates but a shorter one is also detected. A similar situation has been previously reported for TSPP interaction with CTAB micelles [43], where biexponential anisotropy decays with times of 11.4 ns (associated with overall motion of the micelle)

**Table 2** Fluorescence anisotropy decay parameters of TSPP (0.7 μM) in aqueous solution at different pH and in the presence of different [BSA], using Eq. 2 ($\lambda_{exc}$=430 nm)

| Sample | $\lambda_{em}$/nm | $r_0$ | $\phi$/ns ($R_H$/Å)[a] | $\chi^2$ |
|---|---|---|---|---|
| TSPP, pH=2.5 | 648 | 0.11 | 0.462 (8) | 1.084 |
| TSPP, pH=7.4 | 648 | 0.09 | 0.400 (8) | 1.097 |
| [BSA]/[TSPP]=10, pH=7.4 | 648 | 0.15 | 46 (37) | 1.034 |
| [BSA]/[TSPP] = 10, pH=2.5 | 648 | 0.152 | 20 (28) | 1.028 |
| | 713 | 0.124 | 20 (28) | 1.013 |

[a] Rotating species hydrodynamic radii obtained using Stokes–Einstein equation

**Fig. 2** Fluorescence anisotropy decays of TSPP (0.7 μM) in the presence of BSA (**a**) at pH=7.4, [BSA]/[TSPP]=10 ($\lambda_{exc}$= 430 nm); and (**b**) at pH=2.5, *1* [BSA]/[TSPP]=0.03; *2* [BSA]/ [TSPP]=10 ($\lambda_{exc}$=480 nm). $\lambda_{em}$=648 nm
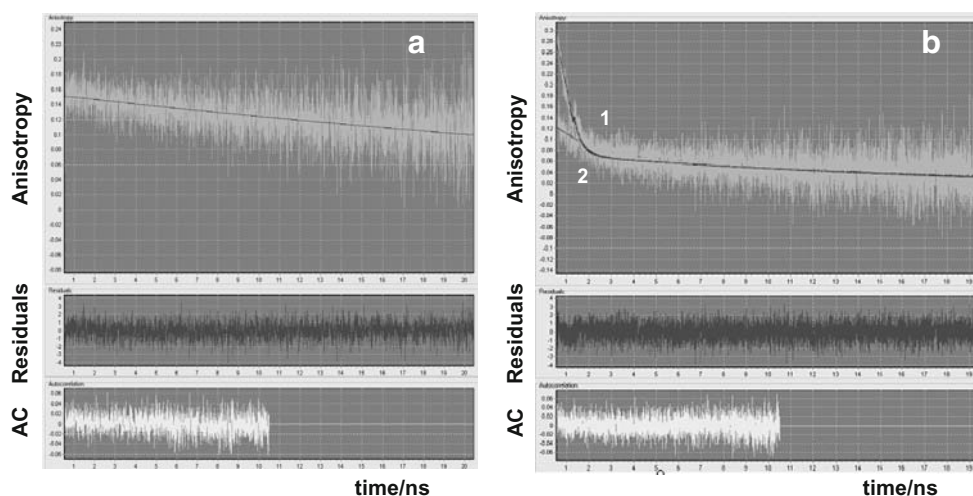


and of 1.52 ns (attributed to the wobbling of the porphyrin in the micelle), were obtained. In the case of the intrinsic probe tryptophan, Trp, several reports on literature have shown a short correlation time (0.5 ns) attributed to fast rotation of the residue involving an angular displacement of Trp as high as 37° [44]. These observations corroborate the idea of local fluidity in proteins.

In this case, we considered a model where the anisotropy $r(t)$ decays to zero because of either rapid reorientation (which occurs in a restricted region within the protein matrix assumed, for simplicity, as a cone), or overall rotation of the protein. For independent segmental and rotational motions the anisotropy may be written as the product of these two contributions, in the following simplified expression [45, 46]:

$$r(t) = \{\beta_1 \exp\left(-t/\phi_{int}\right) + \beta_2\} \exp\left(-t/\phi_{prot}\right) \quad (3)$$

where $\phi_{int}$ and $\phi_{prot}$ are the time constants for the rapid internal motion and for the overall rotation of BSA, respectively, and $\beta_1+\beta_2$ is the initial anisotropy $r_0$. We can also define the square of order parameter $S^2$ which is a measure of the equilibrium orientational distribution of the probe) for the porphyrin in the protein, $S^2=\beta_2/r_0= 0.5\cos\theta_c(1+\cos\theta_c)$, and from which the cone semi-angle $\theta_c$ may be obtained.

This model was then applied to the situation at high [BSA]/[TSPP] upon excitation at 480 nm (see Fig. 2b). The anisotropy decays obtained were very well fitted with $\phi_{prot}$= 23 ns (in agreement with the value obtained at $\lambda_{exc}$= 430 nm), and $\phi_{int}$=1.2 ns.

For a random distribution of orientations, as in liquids, the value for the order parameter is zero, and for orientationally ordered systems $S$ is maximum at 1. Therefore, the order parameter $S$=0.78 ($\theta_c$=44°) indicates that the equilibrium orientational distribution is rather constrained. While this parameter indicates the spatial constraint for the motion of

the molecule within the protein matrix, the value of diffusion coefficient of internal motion indicates the dynamics of the molecule in the restricted space. The value of $D_w=(1-S^2)/ 6\phi_{int}=0.5\times10^8$ s$^{-1}$, is ca. 7 times less than the rotational diffusion coefficient for TSPP in water where the wobbling is free ($S^2$=0).

Similar values of the order parameter ($S$=0.72) and $D_w$= $0.7\times10^8$ s$^{-1}$ were reported for protoporphyrin IX in aqueous micelles of Triton X-100 [47].

At low [BSA]/[TSPP], when porphyrin J-aggregation prevails the decays are never single exponential whatever the excitation/emission conditions used. Upon excitation at 430 nm (monomer absorption) the decays are biexponential, where a short correlation time predominates ($\phi$=0.4 ns). From data showed above, this value may safely be assigned to TSPP monomer rotation free in aqueous solution, whereas the long correlation time ($\phi$=20 ns) comes from some TSPP already bound to BSA. The rotational reorientation time for the large J-aggregate cannot be determined because the fluorescence lifetime is not long enough to follow slow rotational tumbling time of such aggregate. However, a striking difference occurs at low [BSA]/[TSPP]: upon excitation at 480 nm independently of the emission wavelength used, $r_0$ is much higher (Fig. 2b) than those obtained for the monomer ($r_0$~0.1, Table 2) or for TSPP/ BSA complex ($r_0$=0.12–0.15, Table 2). The heterogeneity of anisotropy decay may be due to the coexistence of multiple rotational modes, global and local motions. The fundamental anisotropy $r_0$ contains information about the angle $\alpha$ between absorption and emission moments, and has a theoretical maximum of 0.4 for fluorescent molecules randomly oriented, which corresponds to parallel dipoles ($\alpha$=0°). However, the maximum value predicted for the case of randomly oriented metalloporphyrins is lower (0.1 [48]) due to $D_{4h}$ symmetry and degeneracy of the excited states, in agreement with the value obtained for TSPP at pH=2.5. On the other hand, literature data also predict in case of J-
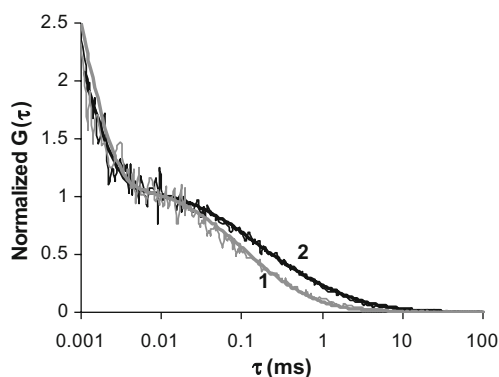
**Fig. 3** Normalized autocorrelations $G(\tau)$ and fitted theoretical curves (*bold lines*) describing a diffusion and triplet state blinking model, of TSPP (10 nM) in the presence of BSA, *1* pH=2.5; *2* pH=7.4 ($\lambda_{exc}=$ 638 nm, $\lambda_{em}=$695AF55 band-pass filter)

aggregates, high initial anisotropies as a result of coherent excitation [49]. A fundamental anisotropy of 0.4 was obtained for TSPP J-aggregate induced by CTAB (exc= 695 nm) together with a very fast anisotropy decay ~40 ps and a "very slow decay" [43]. The latter was indicative of the aggregate large size whereas the former was attributed to an electronic dephasing process.

*Fluorescence correlation spectroscopy* Normalized autocorrelation traces (experimental and fitted) of TSPP and TSPP in the presence of BSA at pH=2.5 and 7.4 are presented in Fig. 3. System calibration was performed by using the red-emitting dye Atto 655 as reference. A diffusion model was sufficient to fit the autocorrelation function calculated for Atto 655, where the shape of the focal volume is approximated by a Gaussian profile with a $1/e^2$ axial ($z_0$) to lateral ($w_0$) dimension ratio $k$ ($k=z_0/w_0$) [50]:

$$G_D(\tau) = \frac{1}{N} \cdot \left(1 + \frac{\tau}{\tau_D}\right)^{-1} \cdot \left(1 + \frac{\tau}{k^2 \tau_D}\right)^{-1/2} \qquad (4)$$

where, $N$ is the mean number of fluorescent molecules within the sample volume and $\tau_D$ is the characteristic diffusion time for a molecule through the effective volume element. FCS can be used to study molecular interactions at low concentrations. The diffusion time $\tau_D$ of a molecule,

when modeled as non-interacting, uncharged spherical particle, is proportional to the square of the beam waist $w_o$, at the focus of the laser beam [51, 52] and allows the determination of the translational diffusion coefficient, $D$ via:

$$\tau_D = \frac{w_D^2}{4D} \qquad (5)$$

If the molecule under study interacts with other molecules, that introduces changes mainly in the particle diameter and therefore leads to an increase in diffusion time. Besides, to account for the fluctuations of TSPP between a fluorescent bright state and a dark triplet state an additional term must be added to the diffusion model [53, 54] which allows to estimate the fraction of molecules in the triplet state ($T$) as well as the triplet state conversion time ($\tau_T$).

$$G_T(\tau) = \left(1 + \frac{T}{1-T} \cdot e^{-\tau/\tau_T}\right) \qquad (6)$$

Since in this case $\tau_D \gg \tau_T$ and the values of D extracted are, within error, independent of the excitation power, then the full correlation curve may be given by $G_{total}(\tau)= G_D(\tau) \times G_{triplet}(\tau)$ [55].

Under the present experimental conditions, i.e., single channel detection, signal "contamination" from detector afterpulsing is inherent. Afterpulsing denotes a nonideal behavior of the detector where an artificial count is generated soon after a real photon pulse. This occurs with a probability that is almost independent of variations in the count rate but characteristic for a given detector [56]. Typical afterpulsing time constants are of the order of a few hundred ns, which make it hard to distinguish from triplet effects. This problem can be minimized by using two detectors and cross-correlating the signals between them since afterpulses from one detector are not correlated to genuine photon detection events of the other detector [54]. In the present case this would imply an unaffordable sacrifice in count rate. A recent method using fluorescence lifetime for separating the true fluorescence from after pulsing events has been proposed [57, 58]. We have not corrected FCS data against after-pulsing, except that in fitting we have ignored the correlation function at delay times below 1 μs.

**Table 3** Translational diffusion times ($\tau_{diff}$) and coefficients ($D$), triplet state conversion times ($\tau_T$), number of molecules ($N$), brightness ($q$) and hydrodynamic radii ($R_H$) of TSPP (3 nM) in aqueous solution at different pH and in the presence of different [BSA] ($\lambda_{exc}=$638 nm)

| Sample | $N$ | $q$/kcounts | $\tau_{diff}$/μs | $D \times 10^{10}$/m$^2$ s$^{-1}$ | $R_H$/Å | $\tau_T$/μs ($T$) |
|---|---|---|---|---|---|---|
| TSPP/Buffer | 6.2 | 0.83 | 234±10 | 2.67±0.30 | 8.9±0.3 | 0.9±0.1 (77%) |
| [BSA]/[TSPP] = 0.03, pH=2.5 | 0.75 | 2.0 | 517±12 | 1.21±0.20 | 20±2 | 1.0±0.2 (36%) |
| [BSA]/[TSPP] = 100, pH=2.5 | 5.8 | 1.1 | 694±18 | 0.90±0.08 | 26±1 | 0.9±0.1 (59%) |
| [BSA]/[TSPP] = 100, pH=7.4 | 5.9 | 1.0 | 962±45 | 0.65±0.05 | 37±2 | 0.9±0.1 (59%) |

For TSPP molecule alone in solution, there is a contribution of 70% of the molecules in the triplet state with $\tau_T$=0.9 µs which decreases for the TSPP molecule associated to albumin ($T$=59%) and to TSPP J-aggregates (36%; Table 3), since in this case energy is dissipated through non-radiative decay.

The diffusion coefficient obtained, $D$=2.7×10$^{-10}$ m$^2$s$^{-1}$ can be related to the hydrodynamic radius ($R_H$) of the molecule by the Stokes–Einstein relationship $D=kT/6\pi\eta R_H$, where $k$ is the Boltzmann constant, and $\eta$ the solution viscosity at temperature $T$. The value of $R_H$=8.9±0.3 Å is in relative good agreement with the value presented in the previous section [34].

Upon increasing albumin concentration the diffusion time decreases (Table 3), indicating formation of slower diffusing species consistent with the expected TSPP association to the protein (85% at [BSA]/[TSPP]=100). However, a dependence of $D$ with the solution pH is detected: at pH=7.4 $D$=(0.65±0.05)×10$^{-10}$ m$^2$s$^{-1}$ in agreement with literature data obtained with mesoporphyrin IX dihydrochloride by FCS, which binds reversibly to HSA ($K_b$=2.5×10$^7$ M$^{-1}$) [59]; whereas at pH=2.5 $D$=(0.90± 0.08)×10$^{-10}$ m$^2$s$^{-1}$, Fig. 3. A similar dependence with pH had already been shown above where rotational correlation times obtained pointed to smaller rotating entities at low pH. It is known that the 3-D structure of the protein influences its mobility and thus the diffusion coefficient making it possible to follow unfolding processes [60]. Moreover, depending on the native structure of the protein, unfolding may lead to elongated structures (usually causing an increase in measured $R_H$) or to more globular forms (usually with smaller $R_H$).

In conditions where [TSPP] is kept constant and [BSA] is extremely reduced such that [BSA]/[TSPP]=0.03 at pH= 2.5, we observed a decrease in the number of fluorescent molecules together with an increase in the molecular brightness (Table 3), $q$, which can be calculated by dividing the average fluorescence count-rate by the number of molecules within the illuminated region [61]. The number of molecules was almost ten times lower than that obtained for free TSPP, but the increase in brightness was only by a factor of 3. To these changes contributed the lower fluorescence quantum yield of TSPP upon self-association [37] and the increase in the absorption cross-section of the aggregated species [62]. In line with this observation, the diffusion time was longer comparatively to that in the absence of protein (Table 3). This is consistent with the self-association process of TSPP J-aggregation at the protein positive surface, under the aforementioned conditions. Nonetheless, the diffusion coefficient was similar but not identical to that obtained for the TSPP–BSA complex at the same low pH. Taking into consideration the differences detected in the CD signal of BSA in the far-UV upon [TSPP] increase, one is tempted to

justify the slight variation in D with changes in BSA conformation.

## Conclusions

We reported here a combination of an ensemble technique with a single molecule technique to study the influence of the aqueous solution pH on the interactions between the drug carrier protein, HSA, and a water-soluble free base porphyrin, TSPP.

The hydrodynamic radius of TSPP–BSA complex at pH= 7.4 obtained from both TRFA and FCS data is very similar and in agreement with literature value. By contrast, the data extracted for the complex established under acidic conditions point to a smaller structure with the porphyrin experiencing some wobbling in the binding site of the protein. These differences with pH are accompanied by a decrease in α-helix content of BSA which is stabilized by the porphyrin (maximal at 1:1 concentration ratio) but not in conditions such that porphyrin J-aggregates prevail. TSPP J-aggregation can also be detected in FCS through an increase in molecular brightness.

These studies highlighted the large flexibility of albumin essential to accommodate quite distinct molecules and to perform its transportation role in the circulatory system. Moreover, the noncovalent interactions with TSPP were shown to play a relevant role in contributing to stabilize a more native form of the protein especially under acidic conditions.

## References

1. Yeagle PL, Albert AD, Egea PF, Rochel N, Birck C, Vachette P, Timmins PA, Moras D (2001) Effects of ligand binding on the association properties and conformation in solution of retinoic acid receptors RXR and RAR. J Mol Biol 307:557–576
2. Xiao B, Heath R, Saiu P, Leiper FC, Leone P, Jing C, Walker PA, Haire L, Eccleston JF, Davis CT, Martin SR, Carling D, Gamblin SJ (2005) Structural basis for AMP binding to mammalian AMP-activated protein kinase. Nature 449:496–U14
3. Bode C, Kovacs IA, Szalay MS, Palotai R, Korcsmaros T, Csermely P (2007) Network analysis of protein dynamics. FEBS Lett 581:2776–2782
4. Zhong DP, Douhal A, Zewail AH (2000) Femtosecond studies of protein-ligand hydrophobic binding and dynamics: human serum albumin. Proc Natl Acad Sci U S A 97:14056–14061
5. Tatikolov AS, Costa SMB (2004) Complexation of polymethine dyes with human serum albumin: a spectroscopic study. Biophys Chem 107:33–49

6. Lang K, Mosinger J, Wagnerova DM (2004) Photophysical properties of porphyrinoid sensitizers non-covalently bound to host molecules; models for photodynamic therapy. Coord Chem Rev 248:321–350

7. Petitpas I, Petersen CE, Ha C-E, Bhattacharya AA, Zunszain PA, Ghuman J, Bhagavan NV, Curry S (2003) Structural basis of albumin–thyroxine interactions and familial dysalbuminemic hyperthyroxinemia. Proc Natl Acad Sci U S A 100:6440–6445

8. Celej MS, Montich GG, Fidelio GD (2003) Protein stability induced by ligand binding correlates with changes in protein flexibility. Protein Sci 12:1496–1506

9. He XM, Carter DC (1992) Atomic structure and chemistry of human serum albumin. Nature 358:209–215

10. Luetscher JA Jr (1939) Serum albumin. II. Identification of more than one albumin in horse and human serum by electrophoretic mobility in acid solution. J Am Chem Soc 61:2888–2890

11. Andrade SM, Costa SMB (2002) Spectroscopic studies on the interaction of a water soluble porphyrin and two drug carrier proteins. Biophys J 82:1607–1619

12. Maiti NC, Mazumdar S, Periasamy N (1998) J- and H- aggregates of porphyrin–surfactant complexes: time-Resolved fluorescence and other spectroscopic studies. J Phys Chem B 102:1528–1538

13. Paulo PMR, Gronheid R, De Schryver FC, Costa SMB (2003) Porphyrin-dendrimer assemblies studied by electronic absorption spectra and time-resolved fluorescence. Macromolecules 36:9135–9144

14. Andrade SM, Costa SMB (2006) Spectroscopic studies of water-soluble porphyrins with protein encapsulated in bis(2-ethylhexyl) sulfosuccinate (AOT) reverse micelles: aggregation versus complexation. Chem Eur J 12:1046–1057

15. Andrade SM, Costa SMB (2002) Aggregation kinetics of meso-tetrakis(4-sulfonatophenyl)porphine in the presence of proteins: temperature and ionic strength effects. J Fluoresc 12:77–82

16. Elson EL (1985) Fluorescence correlation spectroscopy and photobleaching recovery. Ann Rev Phys Chem 36:379–406

17. Heikal AA, Hess ST, Webb WW (2001) Multiphoton molecular spectroscopy and excited-state dynamics of enhanced green fluorescent protein (EGFP): acid–base specificity. Chem Phys 274:37–55

18. van den Berg PAW, Widengren J, Hink MA, Rigler R, Visser AJWG (2001) Fluorescence correlation spectroscopy of flavins and flavoenzymes: photochemical and photophysical aspects. Spectrochim Acta A 57:2135–2144

19. Carter DC, Ho JX (1994) Structure of serum albumin. Adv Protein Chem 45:153–196

20. Vogel AI (1978) Textbook of quantitative inorganic analysis, 4th edn. Longman, London

21. Bychkova VE, Berni R, Rossi GL, Kutyshenk VP, Ptitsyn OB (1992) Retinol-binding protein is in the molten globule state at low pH. Biochemistry 31:7566–7571

22. Kudryashova EV, Visser AJWG, van Hoek A, de Jongh HHJ (2007) Molecular details of ovalbumin-pectin complexes at the air/water interface: a spectroscopic study. Langmuir 23:7942–7950

23. Digris AV, Skakoun VV, Novikov EG, van Hoek A, Claiborne A, Visser AJWG (1999) Thermal stability of a flavoprotein assessed from associative analysis of polarized time-resolved fluorescence spectroscopy. Eur Biophys J 28:526–531

24. Dertinger T, Pacheco V, von der Hocht I, Hartmann R, Grego I, Enderlein J (2007) Two-focus fluorescence correlation spectroscopy: a new tool for accurate and absolute diffusion measurements. ChemPhysChem 8:433–443

25. Dockal M, Carter DC, Ruker F (2000) Conformational transitions of the three recombinant domains of human serum albumin depending on pH. J Biol Chem 275:3042–3050

26. Chen YH, Yang JT, Chau KH (1974) Determination of helix and beta-form of proteins in aqueous solution by circular dichroism. Biochemistry 13:3350–3359

27. El Kadi N, Taulier N, Le Huerou JY, Gindre M, Urbach W, Nwigwe I, Kahn PC, Waks M (2006) Unfolding and refolding of bovine serum albumin at acid pH: ultrasound and structural studies. Biophys J 91:3397–3404

28. Kuwajima K (1989) The molten globule state as a clue for understanding the folding and cooperativity of globular-protein structure. Proteins 6:87–103

29. Dobson CM (1994) Protein folding. Solid evidence for molten globules. CurrBiol 4:636–640

30. Muzammil S, Kumar Y, Tayyab S (1999) Molten globule-like state of human serum albumin at low pH. Eur J Biochem 266:20–32

31. Qiu W, Zhang L, Obkobiah O, Yang Y, Wang L, Zhong D, Zewail AH (2006) Ultrafast solvation dynamics of human serum albumin: correlations with conformational transitions and site-selected recognition. J Phys Chem B 110:10540–10549

32. Goto Y, Takahashi N, Fink AL (1990) Mechanism of acid-induced folding of proteins. Biochemistry 29:3480–3488

33. Matulis D, Baumann CG, Bloomfield VA, Lovrien RE (1999) 1-Anilino-8-naphthalene sulfonate as a protein conformational tightening agent. Biopolymers 49:451–458

34. Maiti NC, Ravikanth M, Mazumdar S, Periasamy N (1995) Fluorescence dynamics of noncovalently linked porphyrin dimers and aggregates. J Phys Chem 99:17192–17197

35. Akins DL, Ozcelik S, Zhu HR, Guo C (1996) Fluorescence decay kinetics and structure of aggregated tetrakis(p-sulfonatophenyl) porphyrin. J Phys Chem 100:14390–14396

36. Mazzaglia A, Angelini N, Darcy R, Donohue R, Lombardo D, Micali N, Sciortino MT, Villari V, Scolaro LM (2003) Novel heterotopic colloids of anionic porphyrins entangled in cationic amphiphilic cyclodextrins: spectroscopic investigation and intra-cellular delivery. Chem Eur J 9:5762–5769

37. Miura A, Shibata Y, Chosrowjan H, Mataga N, Tamai N (2006) Femtosecond fluorescence spectroscopy and near-field spectroscopy of water-soluble tetra(4-sulfonatophenyl)porphyrin and its J-aggregate. J Photochem Photobiol A Chem 178:192–200

38. Castellano FN, Dattelbaum JD, Lakowicz JR (1998) Long lifetime Ru(II) complexes as labeling reagents for sulfhydryl groups. Anal Biochem 255:165–170

39. Ferrer ML, Duchowicz R, Carrasco B, de la Torre JG, Acuna AU (2001) The conformation of serum albumin in solution: a combined phosphorescence depolarization-hydrodynamic modeling study. Biophys J 80:2422–2430

40. Marzola P, Gratton E (1991) Hydration and protein dynamics: frequency domain fluorescence on proteins in reverse micelles. J Phys Chem 95:9488–9495

41. Lakowicz JR, Gryzynski I (1992) Tryptophan fluorescence intensity and anisotropy decays of human serum albumin resulting from one photon and two-photon excitation. Biophys Chem 45:1–6

42. Bloomfield VA (1966) The structure of bovine serum albumin at low pH. Biochemistry 5:684–689

43. Maiti NC, Mazumdar S, Periasamy N (1998) J- and H-aggregates of porphyrins with surfactants: fluorescence, stopped-flow and electron microscopy studies. J Porph Phthalc 2:369–376

44. Lakowicz JR, Maliwal BP, Cherek H, Balter A (1983) Rotational freedom of tryptophan residues in proteins and peptides. Biochemistry 22:1741–1752

45. Lipari G, Szabo A (1980) Effect of librational motion on fluorescence depolarization and nuclear magnetic-resonance relaxation in macromolecules and membranes. Biophys J 30:489–506

46. Visser AJWG, Vos K, van Hoek A, Santema JS (1988) Time-resolved fluorescence depolarization of rhodamine B and (octadecyl)rhodamine B in Triton X-100 micelles and aerosol OT reversed micelles. J Phys Chem 92:759–765

47. Maiti NC, Mazumdar S, Periasamy N (1995) Dynamics of porphyrin molecules in micelles—picosecond time-resolved fluorescence anisotropy studies. J Phys Chem 99:10708–10715

48. Gouterman M, Stryer L (1962) Fluorescence polarization of some porphyrins. J Chem Phys 37:2260–2265
49. Galli C, Wynne K, Lecours SM, Therien MJ, Hochstrasser RM (1993) Direct measurement of electronic dephasing using anisotropy. Chem Phys Lett 206:493–499
50. Rigler R, Mets U, Widengren J, Kask P (1993) Fluorescence correlation spectroscopy with high count rate and low-background—analysis of translational diffusion. Eur Biophys J 22:169–175
51. Elson EL, Madge D (1974) Fluorescence correlation spectroscopy.1. Conceptual basis and theory. Bioploymers 13:1–27
52. Haupts U, Maiti S, Schwille P, Webb WW (1998) Dynamics of fluorescence fluctuations in green fluorescent protein observed by fluorescence correlation spectroscopy. Proc Natl Acad Sci U S A 95:13573–13578
53. Schwille P (2001) Fluorescence correlation spectroscopy and its potential for intracellular applications. Cell Biochem Biophys 34:383–408
54. Widengren J, Mets U, Rigler R (1995) Fluorescence correlation spectroscopy of triplet-states in solution—a theoretical and experimental study. J Phys Chem 99:13368–13379
55. Novo M, Felekyan S, Seidel CAM, Al-Soufi W (2007) Dye-exchange dynamics in micellar solution studied by fluorescence correlation spectroscopy. J Phys Chem B 111:3614–3624
56. Höbel M, Ricka J (1994) Dead-time and afterpulsing correction in multiphoton timing with nonideal detectors. Rev Sci Instrum 65:2326–2336
57. Enderlein J, Gregor I (2005) Using fluorescence lifetime for discriminating detector afterpulsing in fluorescence correlation spectroscopy. Rev Sci Instrum 76:033102
58. Kapusta P, Wahl M, Benda A, Hof M, Enderlein J (2007) Fluorescence lifetime correlation spectroscopy. J Fluoresc 17:43–48
59. Modos K, Galaantai R, Baardos-Nagy I, Wachsmuth M, Toth K, Fidy J, Langowski J (2004) Maximum-entropy decomposition of fluorescence correlation spectroscopy data: application to liposome-human serum albumin association. Eur Biophys J 33:59–67
60. Chattopadhyay K, Saffarian S, Elson EL, Frieden C (2005) Measuring unfolding of proteins in the presence of denaturant using fluorescence correlation spectroscopy. Biophys J 88:1413–1422
61. Haustein E, Schwille P (2003) Ultrasensitive investigations of biological systems by fluorescence correlation spectroscopy. Methods 29:153–166
62. Collini E, Ferrante C, Bozio R (2005) Strong enhancement of the two-photon absorption of tetrakis(4-sulfonatophenyl)porphyrin diacid in water upon aggregation. J Phys Chem B 109:2–5